Mon. Not. R. Astron. Soc. **000**, 1–14 (2014) Printed 3 June 2014 (MN LATEX style file v2.2)

V473 Lyrae, a unique second-overtone Cepheid with two modulation cycles

L. Molnár[1,2⋆], L. Szabados[1]
[1] *Konkoly Observatory, Research Centre for Astronomy and Earth Sciences*
Konkoly Thege Miklós út 15-17, H-1121 Budapest, Hungary
[2] *Institute of Mathematics and Physics, Savaria Campus, University of West Hungary*
Károlyi Gáspár tér 4, H-9700 Szombathely, Hungary

arXiv:1406.0494v1 [astro-ph.SR] 2 Jun 2014

Accepted

ABSTRACT
V473 Lyrae is the only Galactic Cepheid with confirmed periodic amplitude and phase variations similar to the Blazhko effect observed in RR Lyrae stars. We collected all available photometric data and some radial velocity measurements to investigate the nature of the modulation. The comparison of the photometric and radial velocity amplitudes confirmed that the star pulsates in the second overtone. The extensive data set, spanning more than 40 years, allowed us to detect a secondary modulation cycle with a period of approximately 5300 days or 14.5 years. The secondary variations can be detected in the period of the primary modulation, as well.

Phenomenologically, the light variations are analogous to the Blazhko effect. To find a physical link, we calculated linear hydrodynamic models to search for potential mode resonances that could drive the modulation and found two viable half-integer (n:2) and three n:4 resonances between the second overtone and other modes. If any of these resonances will be confirmed by non-linear models, it may confirm the mode resonance model, a common mechanism that can drive modulations both in RR Lyrae and Cepheid stars.

Key words: stars: variables: Cepheids – stars: individual: V473 Lyrae

1 INTRODUCTION

V473 Lyrae (HR 7308, $19^{\rm h}15^{\rm m}59\overset{\rm s}{.}49$ $+27^\circ55'34\overset{''}{.}6$, J2000.0) is one of the most peculiar stars among Cepheids. Its light variations were first noted by Breger (1969). Independently, Percy, Baskerville & Trevorrow (1979) identified the star as a short-period Cepheid with a tentative period of 3.04 days. Shortly after, an extensive radial velocity (RV) measurement series confirmed that the true pulsation period is half of the above value, 1.49 days (Burki & Mayor 1980a,b), the shortest value among Galactic Cepheids. Burki & Mayor discovered strong variations in the pulsation amplitude over the one and half years of observations. They concluded that the star either produced a sporadic or even unique event and it is perhaps arriving to the edge the instability strip or, were the variations periodic, it shows something similar to the Blazhko effect observed in RR Lyrae stars.

In the latter case V473 Lyrae would become the first Cepheid to undergo periodic amplitude modulations, with a period longer than two years. Extensive observations finally revealed that the star indeed shows periodic amplitude variations on a time scale of approximately three years (Percy & Evans 1980). The modulation period was determined to be somewhere around 1210 and 1258 days (Breger 1981; Cabanela 1991). The origin of the modulation, however, remained a mystery.

Several mechanisms were proposed during the years, but none of them was found to be satisfactory. Breger (1981) proposed the beating of two closely spaced pulsation frequencies, the cycle length would, however, require a non-radial mode very close to the main mode. Burki (1984) showed that V473 Lyrae has no companions that could cause the amplitude variations. Beating and mode interactions were revisited by Van Hoolst & Waelkens (1995) and Breger (2006). Auvergne (1986) calculated one-zone models with variable external flux to explain the modulation but found that the modulation period should increase over time.

Finally, based on the apparent similarities to the modulation seen in RR Lyrae stars, the Blazhko effect was considered by several authors. Based on the *Hipparcos* light curve, Koen (2001) found that the pulsation amplitude is strongly modulated with a period of about 1200 days but did not detect phase variations. Burki (2006) did find changes in the pulsation phase, but he argued that the star exhibits discrete

⋆ E-mail: molnar.laszlo@csfk.mta.hu

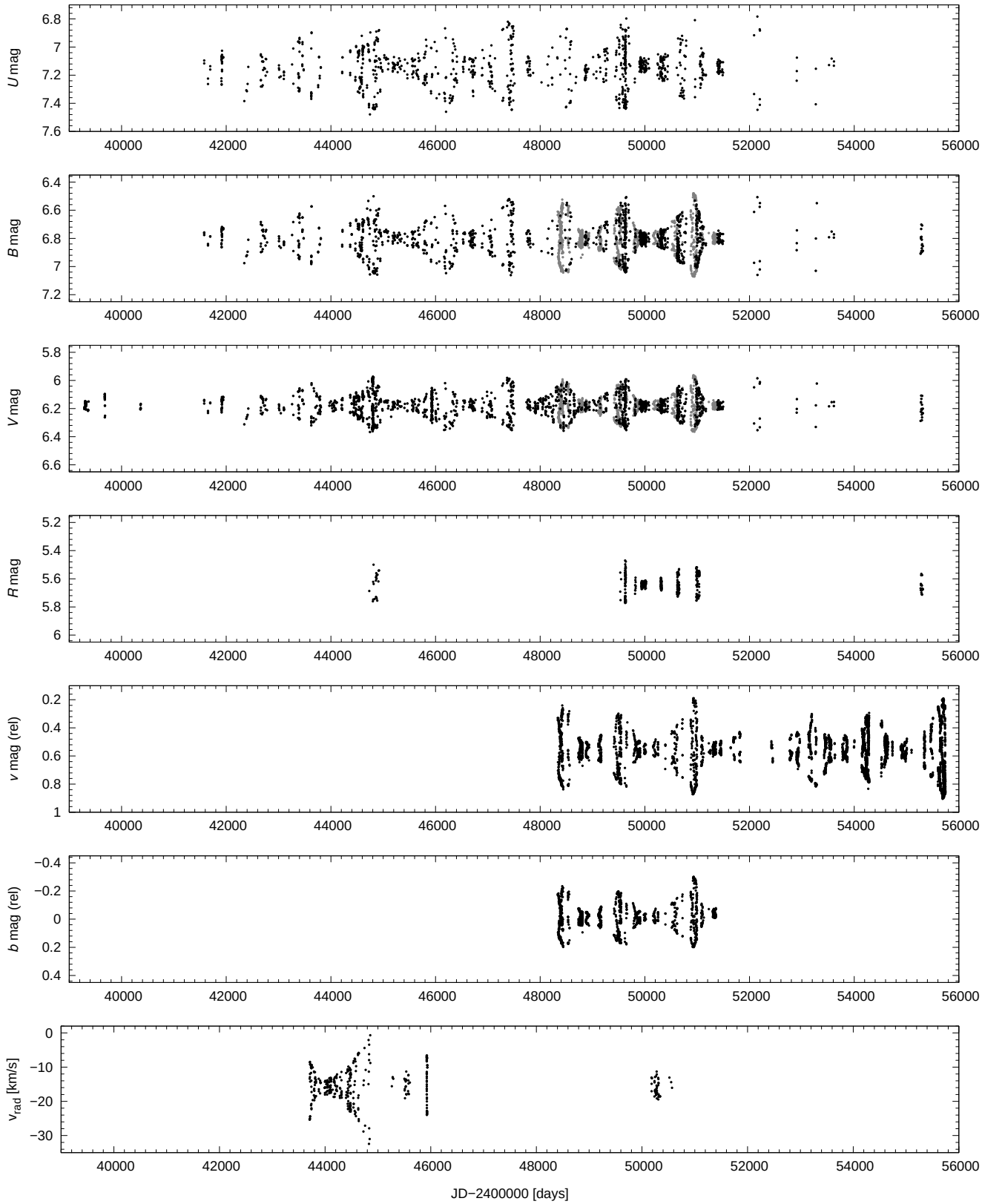

Figure 1. Observed variations of V473 Lyrae. First four rows: Johnson *UBVR* photometric data. Black: original data; grey: transformed from the Strömgren colours. The I band contains very few points hence I data have not been plotted. Rows five and six: Light curve in Strömgren v and b bands. The u and y bands have the same sampling as the b band and are omitted too. The last row displays the RV variations. The modulation is evident in all cases.

phase jumps instead of the more gradual phase modulation. Stothers (2009) argued that the Blazhko effect in RR Lyrae stars and Cepheids might be driven in a very similar manner by turbulent convective cycles. A detailed, direct comparison with the RR Lyrae stars, however, has not been carried out so far. Admittedly, since there is no accepted explanation for the Blazhko effect yet, the comparison can only be phenomenological. But any similarities or differences could provide additional clues and constraints for a common mechanism that may operate in both types of variables.

New observational and theoretical developments fundamentally changed the way we look at the Blazhko effect in RR Lyrae stars (Szabó 2014). Space-based photometry revealed additional modes and resonances in the modulated stars, features that all their stable siblings, so far, lack (Benkő et al. 2010). The modulation itself was found to be non-repetitive or even extremely variable in several stars (Guggenberger et al. 2012). Moreover, observational findings contradict most proposed mechanisms for the Blazhko effect. The most likely explanation is currently the mode resonance hypothesis (Buchler & Kolláth 2011). Unlike in the non-radial resonant rotator model, the modulation arises from the non-linear interaction of the modes instead of the rotation of the star.

The mode resonance model can be applied to Cepheids too. These stars show the same dynamic features that were observed in RR Lyrae stars: multi-mode pulsation, period doubling and strange modes, modes trapped close to the surface (Moskalik & Buchler 1990; Buchler et al. 1997; Smolec et al. 2012). Therefore we expect that mode resonances may occur in these stars as well. However, modulated Cepheids are much rarer than modulated RR Lyrae stars. The notable exceptions are the double-mode Cepheids in the Large Magellanic Cloud but in those stars both modes show periodic amplitude and phase variations (Moskalik & Kołaczkowski 2009). Among the Galactic Cepheids, V473 Lyrae was the only definitive case, until the recent announcement of a few additional stars with indications of Blazhko-like amplitude variability by Engle & Guinan (2013).

We started investigating V473 Lyrae to find out if the modulation properties are truly similar to the Blazhko effect in RR Lyrae stars. Our first results were promising: we showed that the star exhibits simultaneous amplitude and phase modulations (Molnár et al. 2013). In this paper we present the results of an in-depth analysis of the multicolour photometric data and some limited RV measurements. In addition we carried out hydrodynamic simulations to search for mode resonances that might be at work in the star.

2 DATA SETS

In order to follow the modulation of V473 Lyrae, we collected all the available observations in Johnson colours of the star[1]. We examined the observations collected by amateur astronomers in the AAVSO database: a handful of photometric measurements were included but scatter of the visual estimates were too large compared to the pulsation amplitude so they were omitted. Most observations were made in the *UBV* bands, but we collected a small amount of *R*- and *I*-band photometry as well. *UBVR* light curves are shown in the first four rows of Fig. 1.

In addition, we acquired the extensive Strömgren-colour observations of the Four College APT (Automatic Photoelectric Telescope) run by the College of Charleston (SC, USA). The latter data set spans a shorter time interval but contains more observations than the Johnson data. The first half of the data is covered by *uvby* multicolour photometry but the second half was observed in *v*-band only. Curiously, the interest in the star declined at the dawn of the 21st century—at about JD 2451500 or late 1999. Apart from a few Johnson measurements, the variations are covered only by the Strömgren *v* observations (Fig. 1).

The multicolour part of the Strömgren photometry can be converted into the Johnson system. According to Williams (1966), the following relation applies to field Cepheids:

$$V = y + 0.028(b - y) - 1.367. \quad (1)$$

Table 1. *UBV* photometric data obtained at the Konkoly Observatory

$JD_\odot$ 2 400 000+	V mag	$B-V$ mag	$U-B$ mag
50252.3594	6.175	0.609	0.263
50281.4811	6.193	0.614	0.329
50609.4014	6.178	0.621	0.343
50633.4003	6.220	0.658	0.316
50634.3635	6.073	0.566	0.295
50956.3977	5.994	0.530	0.280
50957.3853	6.328	0.661	0.362
50960.3980	6.314	0.661	0.303
50961.3615	6.249	0.675	0.300
51051.3351	6.203	0.612	0.303
51052.2981	6.232	0.649	0.334
52086.4270	6.031	0.558	0.208
52087.3843	6.288	0.663	0.264
52150.4565	5.967	0.517	0.180
52151.3126	6.336	0.701	0.290
52195.2715	6.005	0.548	0.202
52196.2477	6.315	0.683	0.294
52197.2143	6.253	0.686	0.313
52198.2225	5.994	0.532	0.238
52902.2449	6.211	0.650	0.259
52904.2392	6.185	0.626	0.241
52906.2333	6.115	0.605	0.236
53266.2687	6.313	0.695	0.280
53267.2642	6.159	0.619	0.257
53286.2548	6.004	0.523	0.208
53518.4131	6.166	0.603	0.240
53569.3638	6.136	0.593	0.234
53612.3055	6.164	0.608	0.242
53614.3085	6.135	0.613	0.235

[1] References to the observations: Percy & Evans (1980); Burki & Mayor (1980b); Breger (1981); Fernie (1982); Burki, Mayor & Benz (1982); Henriksson (1983); Arellano Ferro (1984); Eggen (1985); Burki et al. (1986); Fabregat, Suso & Reglero (1990); Arellano Ferro et al. (1990); ESA (1997); Kiss (1998); Ignatova & Vozyakova (2000); Breger (2006); Berdnikov (2008) and references therein; Oja (2011); Usenko (private comm.); Szabados (this paper, Table 1); AAVSO.

Table 2. Available data sets. Columns: data type, photometric colour or RV; net number of points; number of points with the transformed Strömgren data added; time range of the data sets. The number of the *uby* data is identical in each band.

Type	No. of points	With added points	JD range
U	1005	–	2441579-2453614
B	1465	2812	2441579-2455312
V	2026	3369	2439289-2455312
R	494	–	2444732-2455312
I	193	–	2444732-2455312
v	4623	–	2448334-2455741
uby	1347	–	2448334-2451356
$v_{\rm rad}$	376	–	2443706-2450568

Cousins & Caldwell (1985) provided additional transformations between the two systems. To obtain the B colour, we used the following relation:

$$(B-V) = 0.929(b-y) + 0.576(v-b) - 0.083. \quad (2)$$

We transformed the Strömgren photometry into Johnson B and V colours with the help of the above equations. The additional points are included in the B and V light curves in Fig. 1 with grey colour. The exact number of data points in each band is given in Table 2. The transformed points and the observations of Oja (2011) are new additions to the B and V colours compared to Molnár et al. (2013).

We also have some RV measurements at our disposal (lowest panel in Fig. 1). Unfortunately, we could not access the extensive measurements shown in Burki (2006). Nevertheless, the limited data set covers most modulation phases.

3 IDENTIFICATION OF THE PULSATION MODE

Being a unique Cepheid in our Galaxy, the pulsation mode of V473 Lyr is a key issue for explaining its peculiar behaviour. Presence of the Blazhko modulation was reported for a number of Cepheid variables in the Large Magellanic Cloud. Such modulation phenomenon only occurs among double-mode Cepheids pulsating simultaneously in the first and second overtone modes (Moskalik & Kołaczkowski 2009).

The earliest discussions on the pulsation mode of V473 Lyr are found in the papers by Burki, Mayor & Benz (1982) and Burki et al. (1986). In the first paper, they determined the pulsation constant, Q, from the pulsation period, mass, and radius of the star, and compared with the theoretical Q value obtained for various modes of oscillation. Their conclusion is that pulsation in the second radial overtone is most probable in the case of V473 Lyr but the first overtone cannot be excluded, either. In their subsequent paper, Burki et al. (1986) derived physical properties of V473 Lyr using three versions of the Baade-Wesselink method, and based on the stellar radius obtained they again concluded that this Cepheid most probably pulsates in the second or higher overtone. The position of V473 Lyr on the period-luminosity plot is also compatible with the overtone pulsation (Fabregat et al. 1990).

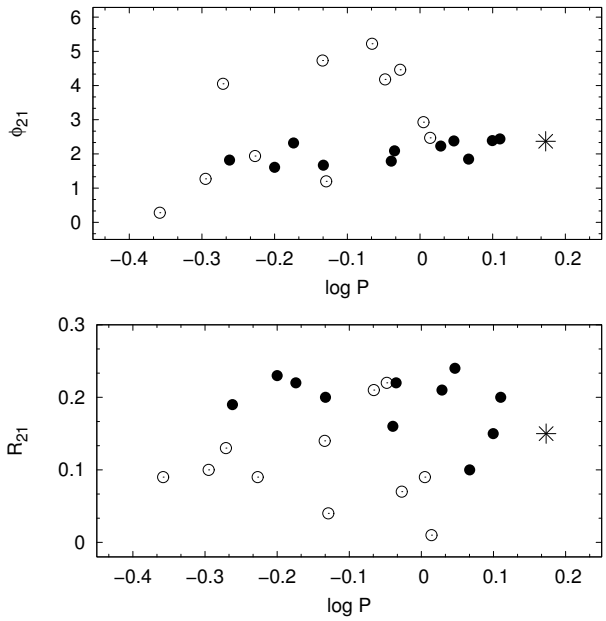

Figure 2. Fourier parameter relations for Galactic double-mode Cepheids versus the logarithm of the pulsation mode period in days. Top panel: the $\phi_{21} = \phi_2 - 2\phi_1$ phase relation; bottom panel the $R_{21} = A_2/A_1$ amplitude relation. Filled points: first overtone; circles: second overtone. The star marks the position of V473 Lyrae. Because of the overlap and the large scatter of the second-overtone points, Fourier parameters alone cannot identify the pulsation mode of V473 Lyrae.

There are, however, other methods for mode identification of Cepheids not applied in the case of V473 Lyr so far. These methods are based on various phenomenological properties (amplitude, shape, phase relations) of the phase curves of the brightness and RV variations.

The most commonly used method of determining the mode of pulsation for a Cepheid is based on the Fourier decomposition of the photometric phase curve. The Fourier coefficients defined by Simon & Lee (1981) show a characteristic progression as a function of the pulsation period. Based on the R_{21} and R_{31} amplitude parameters and ϕ_{21} and ϕ_{31} phase parameters the overtone pulsators are clearly separated from Cepheids pulsating in the fundamental mode (for Cepheids in the Small Magellanic Cloud see Figures 2-3 in Soszyński et al. 2010). However, Cepheids pulsating in the first two overtone modes are partly overlap in the Fourier parameter vs. pulsation period diagrams. In the case of Magellanic Cepheids, the distinction between first- and second-overtone pulsators can be made by their position in the period vs. apparent brightness (or Wesenheit magnitude) graphs, because all Cepheids situated in either Magellanic Cloud are practically at the same distance from us. This is not a viable alternative for Galactic Cepheids because they are at various distances.

The available Fourier parameter vs. period diagrams for Galactic Cepheids only involve fundamental and first-overtone pulsators and no single-period, second-overtone Galactic Cepheid is known with certainty. There are, however, 11 known double-mode Cepheids in our Galaxy which pulsate simultaneously in first and second overtones

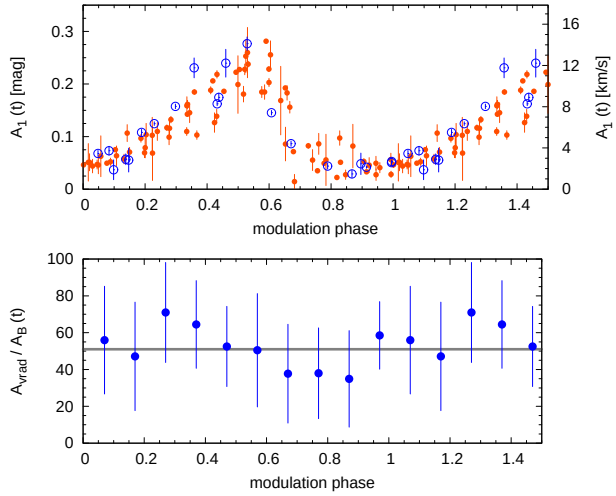

Figure 3. Upper panel: the amplitude variations of the B passband (orange dots) and RV data (blue circles), scaled together and folded with the primary modulation period. Lower panel: the $q = A_{V_{\rm rad}}/A_B$ scaling factor, calculated for 10 phase bins. The average (grey line) is 51, indicating that the star pulsates in the second overtone.

(V363 Cas, V1048 Cen, V767 Sgr, ASAS 062735+0949.8, ASAS 064135+0756.6, ASAS 074343-2050.3, ASAS 083434-4134.6, ASAS 131714-6605.0, ASAS 142346-5829.4, ASAS 191351+0251.3, and NSVS 2030690). To perform a Fourier decomposition of their light curves, the photometric data available in the online data bases ASAS (Pojmanski 2002) and NSVS (Wozniak et al. 2004) have been analyzed. The Fourier decomposition was performed using the program package MUFRAN (Csubry & Kolláth 2004). The frequency values of the first and second overtones, f_1 and f_2, were taken from the literature, and the following harmonics and linear combinations of these two basic frequencies were taken into account in the fitting procedure: f_1, $2f_1$, $3f_1$, f_2, $2f_2$, f_1+f_2, $2(f_1+f_2)$, f_2-f_1, $2f_1+f_2$. Inclusion of further frequency components would have been meaningless in view of their negligible amplitudes and the quality of the photometric data sets. The frequencies listed above were fitted simultaneously, and than the R_{21} and ϕ_{21} parameters were derived. The resulting R_{21} vs. $\log P$ and ϕ_{21} vs. $\log P$ diagrams are shown in Fig. 2. In these figures filled circles denote the respective Fourier parameter for the 1st overtone of the Galactic beat Cepheids, while open circles represent the corresponding value for the 2nd overtone oscillations. A star symbol shows the position of V473 Lyrae in both diagrams. Unfortunately, the quality of the available photometric data does not permit a reliable determination of the R_{31} and ϕ_{31} parameters for the Galactic double-mode Cepheids.

Figure 2 indicates partial overlapping of the Fourier parameters for the first and second overtone pulsations in Galactic Cepheids, similarly to the case of Magellanic Cepheids. The position of V473 Lyrae in these diagrams does not prefer either overtone mode, though excludes fundamental-mode pulsation.

There are two methods of mode determination utilizing both photometric and RV measurements. On the one hand, the first-order phase lag between the decomposed RV and photometric curves ($\phi_{21}^{V_{\rm r}} - \phi_{21}^{\rm mag}$) is a good indicator of the pulsation mode, at least for differentiating between fundamental-mode and 1st overtone Cepheids (Ogłoza et al. 2000). This method is only applicable for pulsation periods longer than 3.5 days, so useless in the case of V473 Lyrae. On the other hand, the ratio of the RV and photometric amplitudes also hints at the mode of pulsation (Balona & Stobie 1979). The ratio of these amplitudes, $q = A_{V_{\rm rad}}/A_B$, is about $30-33$ for fundamental-mode Cepheids and $q \approx 35-40$ for Cepheids oscillating in the first overtone (Klagyivik & Szabados 2009). For higher overtones q is even larger. The q parameter is about 51 ± 10 for V473 Lyrae, (the largest value among Galactic Cepheids), although the modulation and the sparse sampling makes the determination somewhat uncertain (Fig. 3 and Sect. 6.3). The ratio is the same for the high and the low-amplitude phases of the long cycle. The unusually high value is a clear evidence that the star is indeed pulsating in the second overtone. We note that Klagyivik & Szabados (2009) warned that binarity could increase the value of the q ratio but the constant time-averaged RV value (Burki 2006) indicates no close-by, high-mass companions.

4 FOURIER ANALYSIS

We investigated the Fourier spectra of all data sets. Spectra from the two best colours, the Johnson B and Strömgren v are plotted in Fig. 4. Since the pulsation frequency is almost 2/3 d^{-1}, ground-based observations of this star suffer from significant aliasing. Daily aliases of the $-f_1$ value from the negative side of the spectrum leak into the positive side at $-f_1+1$ d^{-1}, $-f_1+2$ d^{-1}, etc. values, among which the $-f_1+2$ d^{-1} value coincides with the $2f_1$ value, as indicated in Fig. 4. Similarly, the $3f_1$ peak coincides with the 3 d^{-1} alias peak. The Strömgren data collected from a single site, suffers more from these problems.

Cepheid light curves are much more sinusoidal than the variations of RR Lyrae stars so the amplitudes of the successive harmonics (integer multiplets of the main frequency) decrease very fast. The first harmonic ($2f_1$) was identified in all but the very sparse I data sets. However, the $3f_1$ peak (or a corresponding side-peak) was only detectable in the B, V and v bands that provide the most extensive temporal coverage. The low-frequency modulation peak (f_m) was identified in most bands, although the exact frequency values were uncertain for the shorter *uby* data sets. The Fourier parameters of the B band data are summarized in Table 3.

4.1 Modulation side-peaks

Amplitude and/or phase variations introduce modulation side-peaks around the main peaks in the frequency spectrum. The exact number and amplitudes of these peaks depend not only on the detection limit but on the details of the modulation process as well. On the one hand, Szeidl & Jurcsik (2009) showed that a sinusoidal signal modulated both in amplitude and phase with a periodic function (e.g. another sine) produces an infinite series of side-peaks with decreasing amplitudes. On the other hand, non-sinusoidal modulation, especially in the pulsation phase, may create more complicated patterns around the main peaks (Benkő, Szabó & Paparó 2011). Hence the number of

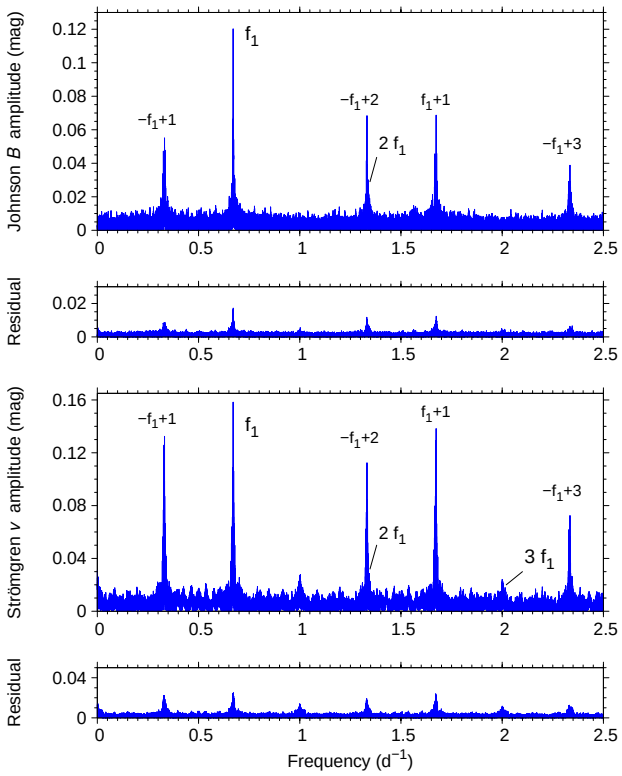

Figure 4. Fourier spectra of the Johnson B and Strömgren v data sets of V473 Lyrae. Real and alias peaks are indicated. The bottom panels show the residual spectra after prewhitening with the frequencies indicated in Fig. 5.

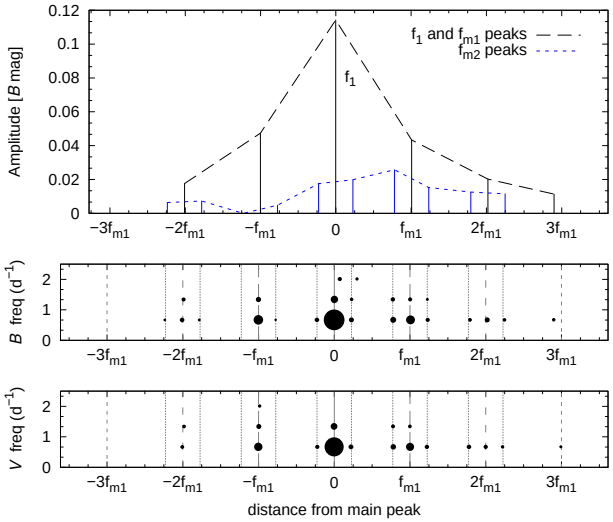

Figure 5. Summary of the detected main frequency peaks and side-peaks, except for the modulation frequencies themselves. Top panel: identified peaks around the pulsation frequency. Black: f_1 and the primary modulation peaks. Blue: secondary modulation peaks and combination peaks. Numerical values are summarized in Table 3. Lower panels: the peaks are plotted similar to an echelle diagram: successive orders of harmonics with the corresponding side-peaks were placed above each other. Point sizes are derived from the amplitudes but the second and third rows of points in both panels are enlarged for better visibility.

side-peaks and the amplitude ratios provide valuable information about the nature of the modulation.

Previous studies only identified triplet components, *e.g.* $f_1 \pm f_m$ side-peaks (Koen 2001; Breger 2006). We detected a single quintuplet peak during the preliminary analysis (Molnár et al. 2013). We repeated the analysis with the extended data sets. After a thorough search we identified side-peaks up to the third order ($f_1 \pm 3f_m$) in different bands. We determined the modulation period to be $P_m = 1205 \pm 3$ days, based on the individual modulation frequencies.

In Fig. 6 we folded the light curves with the modulation and pulsation periods, respectively. The strong amplitude variations can be clearly seen. Interestingly, the modulation cycle is very asymmetric (left panel of Fig. 6): the increase of the amplitude lasts much longer than the fast decrease which is then followed by an extended phase in amplitude minimum. In contrast, the Blazhko effect in RR Lyrae stars is relatively symmetric, although some stars do show some asymmetry (Benkő et al. 2010; Skarka 2014).

We also checked the colour dependence of the ratio of the pulsation and modulation peaks. We used the multicolour part of the Strömgren data set. The ratio turned out to be constant in all four passbands so the modulation does not exhibit any colour dependence (Fig. 7).

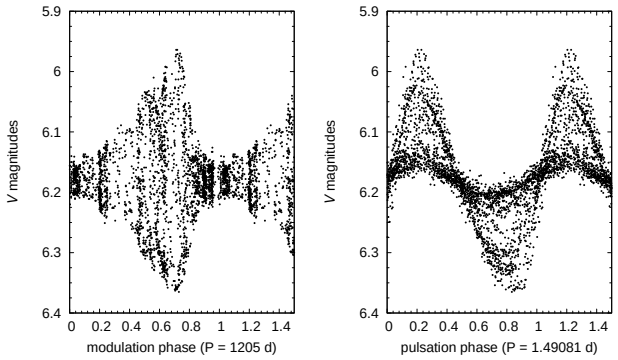

Figure 6. Johnson V band light curves, folded with the modulation and pulsation periods. The modulation is not symmetric: the pulsation amplitude decreases much faster than it increases. Because of the additional variations (the secondary modulation, see Sect. 5.1), we only used data between JD 2447700 and 2451500 in this plot.

4.2 Residual power

Interestingly, significant power remained in the spectra even after removing all side-peaks (lower panels of Fig. 4). One can of course continue to prewhiten those structures: overlapping multiplet structures were already observed in RR Lyrae stars with multiple or changing modulation cycles (Sódor et al. 2011; Guggenberger et al. 2012). Cabanela (1991) already reported that the modulation seems not to be perfectly periodic. Further inspection revealed a regular structure of additional side-lobes around some of the main peaks and primary modulation side-peaks. Such pattern can be interpreted as a secondary modulation superimposed on the first one. Most additional peaks are only slightly farther from the primary modulation peaks than the first side-peak of the window function, *viz.* $f_{m2} \sim 0.00018 - 0.00019\,\mathrm{d}^{-1}$

Table 3. Fourier solution of the Johnson B data set. We used the Period04 and MuFrAn tools throughout our analysis (Lenz & Breger 2005; Csubry & Kolláth 2004). Uncertainties were calculated with the Monte–Carlo simulation of Period04. The original B-band spectrum and the residual after prewhitening with the main peaks and primary side-peaks can be seen in Fig. 4.

Peak	f d^{-1}	A mag	ϕ $\frac{\mathrm{rad}}{2\pi}$	$\sigma(f)$ d^{-1}	$\sigma(A)$ mag	$\sigma(\phi)$ $\frac{\mathrm{rad}}{2\pi}$
Main peaks						
f_{m1}	0.000856	0.009	0.779	0.000018	0.010	0.029
f_1	0.670784	0.114	0.060	0.000003	0.005	0.007
$2f_1$	1.341571	0.017	0.333	0.000029	0.004	0.040
$3f_1$	2.01242	0.005	0.75	0.00098	0.003	0.15
Side-peaks of the primary modulation						
f_1-2f_{m1}	0.66912	0.018	0.83	0.00060	0.011	0.23
f_1-f_{m1}	0.669954	0.047	0.235	0.000005	0.004	0.015
f_1+f_{m1}	0.671620	0.043	0.532	0.000063	0.012	0.043
f_1+2f_{m1}	0.672462	0.020	0.633	0.000012	0.006	0.068
f_1+3f_{m1}	0.67319	0.011	0.52	0.00173	0.008	0.36
$2f_1-2f_{m1}$	1.339919	0.007	0.404	0.000019	0.004	0.052
$2f_1-f_{m1}$	1.34074	0.011	0.60	0.00424	0.013	0.28
$2f_1+f_{m1}$	1.34240	0.007	0.01	0.00049	0.173	0.17
$3f_1+f_{m1}$	2.01260	0.003	0.80	0.02004	0.003	0.34
Side-peaks of the secondary modulation						
f_1-f_{m2}	0.670595	0.018	0.566	0.000019	0.004	0.071
f_1+f_{m2}	0.670973	0.020	0.062	0.000014	0.004	0.039
$2f_1+f_{m2}$	1.34176	0.006	0.34	0.00026	0.003	0.17
Combination peaks						
$f_1-2f_{m1}-f_{m2}$	0.66893	0.006	0.86	0.00242	0.011	0.18
$f_1-2f_{m1}+f_{m2}$	0.66931	0.007	0.136	0.00073	0.007	0.083
$f_1-f_{m1}+f_{m2}$	0.67014	0.005	0.456	0.00007	0.004	0.092
f_1+f_{m1}-f_{m2}	0.67143	0.026	0.15	0.00181	0.025	0.24
$f_1+f_{m1}+f_{m2}$	0.671809	0.015	0.486	0.000031	0.021	0.071
$f_1+2f_{m1}-f_{m2}$	0.672273	0.013	0.319	0.000020	0.011	0.046
$f_1+2f_{m1}+f_{m2}$	0.672650	0.012	0.565	0.000046	0.006	0.059
$2f_1+f_{m1}-f_{m2}$	1.34221	0.008	0.67	0.00218	0.005	0.33
$2f_1+f_{m1}+f_{m2}$	1.34259	0.004	0.97	0.01554	0.171	0.39

compared to $f_{\mathrm{wpeak}} = 0.00014 - 0.00017\,\mathrm{d}^{-1}$. The f_2 frequency we identified in the preliminary analysis is also part of this structure (Molnár et al. 2013). We concluded that the remaining power comes from additional variations with time scales comparable to the length of the data set. The average distance of the secondary side-peaks is $f_{m2} = 0.0001890 \pm 0.0000035\,\mathrm{d}^{-1}$, corresponding to a period of 5290 ± 96 days. The detected peaks in the Johnson B and V colours are summarized in Fig. 5. Note that although the primary modulation peaks form a relatively symmetric structure, the amplitudes of the f_{m2} do not. The highest peak appears next to the $f_1 + f_{m1}$ frequency while we found the lowest peaks (with one non-detection) around the $f_1 - f_{m1}$ frequency. The frequencies derived from the Johnson B data set that provided the highest signal-to-noise ratios, are summarized in Table 3.

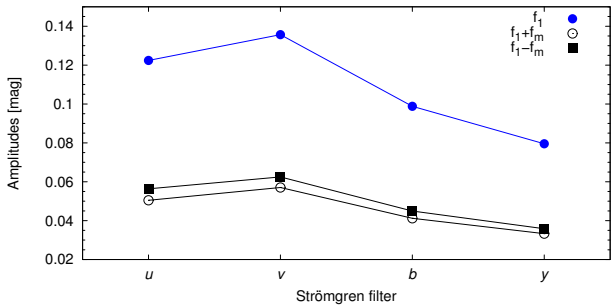

Figure 7. Amplitudes of the f_1 main pulsation peak and the $f_1 \pm f_m$ triplet modulation side-peaks in each Strömgren band. The ratio of the pulsation and modulation peaks is the same in each bandpass.

5 AMPLITUDE AND PHASE VARIATIONS

The large residuals in the Fourier spectra indicate that the modulation of the star may be variable. Preliminary analysis indicated that the star indeed shows changes in the modulation (Molnár et al. 2013). We divided the data sets into bins with lengths between 10 and 100 days, depending on the distribution of the points. Although the pulsation amplitude is higher in the B band, we used the Johnson V data for this analysis because of its better temporal coverage. The pulsation frequency was set to $f_1 = 0.670775\,\mathrm{d}^{-1}$, adopted from the ephemeris used by Berdnikov & Pastukhova (1994). If the temporal coverage allowed, we fitted the amplitude and phase (A_2, ϕ_2) of the $2f_1$ frequency as well. However, the ϕ_2 value was very uncertain in all but the highest-amplitude phases, therefore we could not calculate the epoch-independent relative Fourier-phases, ϕ_{21} and ϕ_{31} (Simon & Lee 1981) for any other parts of the light curve. The ϕ_3 parameter was barely detectable for ther entire data set. Because of this, we resorted to use ϕ_1 itself in the analysis. The results are shown in Fig. 8. We derived the B-band and RV amplitudes in the same way to identify the mode of the pulsation in Sect. 3.

It is clear that both the amplitude and the phase are modulated with the $P_m = 1205 \pm 3$ day period. The variations of the amplitude repeat fairly regularly with slight changes in the maximum modulation amplitude. On the other hand, the phase shows much more complex changes. Significant additional variations occur on about $2 - 4$ modulation-cycle-long time scales.

5.1 Evidence of a secondary modulation cycle

Although the Blazhko-like modulation in a Cepheid is in itself a unique feature, the light variations of the star turned out to be even more complex. The residual power in the Fourier spectra (Fig. 4) and the long-term changes in the phase variation curve (Fig. 8) already indicated that additional variation may be present in the star. The times of maximum pulsational amplitude also seem to deviate from the predicted times in the top panel of Fig. 8.

Further investigation of the phase variation revealed two additional variations (Fig. 9). A secular period change of $\dot{P} = -0.01673 \pm 0.00058$ s/yr $= (-5.30 \pm 0.18) \cdot 10^{-10}$ s/s is present, indicating evolutionary effects. Note that the phase

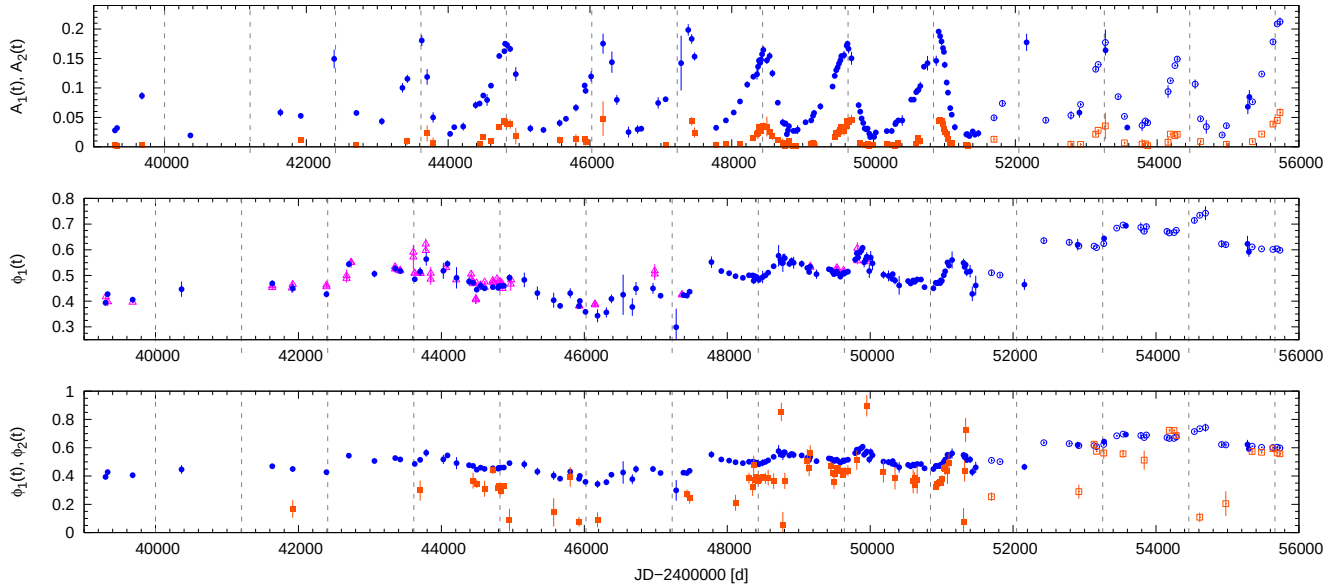

Figure 8. Amplitude and phase variations of V473 Lyrae. Top panel: amplitudes of the $f_1 = 0.670775\,\mathrm{d}^{-1}$ (blue dots) and $2f_1$ (orange squares) peaks. Middle panel: phases of the f_1 peaks (blue), purple triangles are from Berdnikov & Pastukhova (1994) and Berdnikov et al. (1997). Units are rad/2π. Lower panel: phases of both frequency peaks. In the case of ϕ_1, points with $\Delta\phi_1 < 0.2$ uncertainty are only shown. Filled and empty points correspond to Johnson V and Strömgren v colours, respectively, v amplitudes were scaled down to match the V amplitudes. Grey vertical lines mark the modulation cycles with a spacing of 1205 days.

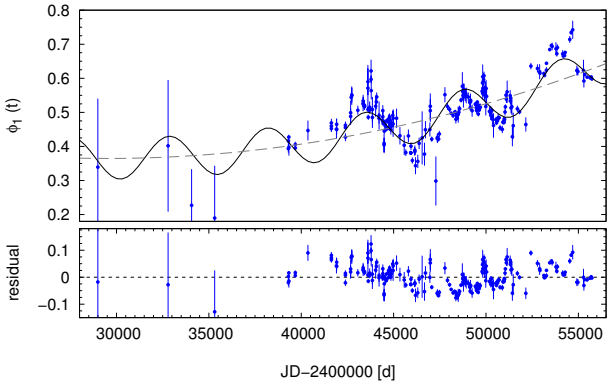

Figure 9. The phase variations fitted with a quadratic term, indicating a shortening pulsation period (the phase variation is the negative of the $O-C$ values), and a sinusoidal with a period of 5290 days. The longer modulation cycle is definitely present in the phase variations. A few early, uncertain points by Berdnikov et al. (1997) are also included.

variations have opposite sign compared to the $O-C$ values hence the quadratic term in Fig. 9 corresponds to a decrease in the average pulsation period.

The second term in Fig. 9 is a sinusoidal function with a period of $P_{m2} = 5290$ d, the value we identified in the Fourier spectra. The amplitude of the variation is $A_\phi(t) = 0.061(\pm0.004)$ rad/2π or $0.091(\pm0.006)$ days. This long-term modulation is clearly different from the faster primary modulation cycle that can be clearly seen in the lower panel of Fig. 9 after removing the two longer variations.

6 DISCUSSION

6.1 Origin of the secondary modulation

A periodic phase modulation could arise from the light-time effect if the star is a member of a binary system. We calculated the approximate mass limit of a companion from the well-known binary mass function:

$$f(m) = 4\pi^2 \frac{(A\,c\sin i)^3}{G\,P^2} = \frac{(M_2 \sin i)^3}{(M_1+M_2)^2} \qquad (3)$$

where A is the semi-amplitude of the $O-C$ or phase variations, c is the speed of light, M_1 and M_2 are the masses of the stars, P is the orbital period, G is the gravitational constant and i is the inclination of the orbit. By setting $P = 5290$ d, $A = 0.091$ d and $M_1 = 4\,M_\odot$ (Fabregat, Suso & Reglero 1990), the calculation yields a mass limit of $M_2 \sin i = 24\,M_\odot$ for a hypothetical companion. However, the delay and the modulation period would mean a RV amplitude of $v_{\rm rad} = 32$ km/s. Neither the last panel in Fig. 1 nor the more extended observations of Burki (2006) show such large variations in the RV measurements. Hence, binarity can be ruled out.

As the secondary phase modulation appeared to be an intrinsic variation of the star, we revisited the light curves to look for corresponding amplitude changes. In Fig. 10 we applied an envelope to the Johnson V data with the same period and phase as that of the secondary phase modulation. The Strömgren v data were scaled to the V data to better visualize the effect. Although the highest-amplitude phases of the primary modulation are missing in several cycles, the envelope curves clearly fit the observations, indicating the presence of the secondary modulation. The peak-to-peak amplitude of the variation is approximately $A_{m2} = 0.09 \pm 0.04$ magnitudes in V colour.

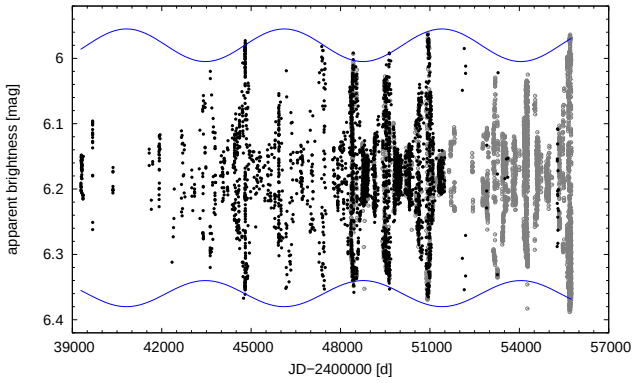

Figure 10. Approximate envelope of the secondary modulation. Black points are the Johnson V, grey circles are the scaled Strömgren v data points. The modulation period is 5290 days (14.5 years).

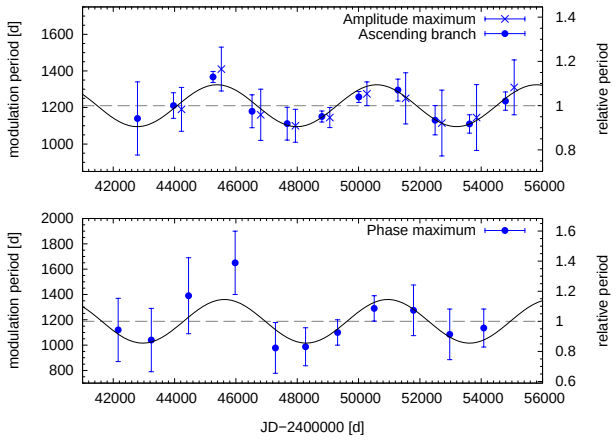

Figure 11. Variations in the cycle length of the primary modulation. Top: based on the $O-C$ variations of the amplitude modulation data (maxima and mean lights of the ascending branch). Bottom: based on the phase modulation data.

Multiple modulation cycles have been already known to exist in some Blazhko RR Lyrae stars (see Sect. 6.4). The primary and secondary cycles can be close to each other, as in the case of CZ Lac where the two cycles were observed close to the 5:4, and in the next season to the 4:3 period ratios (Sódor et al. 2011). The period ratio of the two variations is $P_{m2}/P_{m1} = 4.4 \pm 0.15$. The uncertainties can accommodate an exact $P_{m2}/P_{m1} = 9{:}2$ ratio but it will take further, long-term monitoring to determine the modulation periods more accurately. This aspect of the modulation of V473 Lyr agrees with the Blazhko effect.

6.2 Relation of the two modulation cycles

Another interesting question is whether the secondary modulation is independent of the primary and affects only the pulsation or the two modulations interact with each other. To answer this, we derived the $O-C$ curves of the modulation. For the phase variation we calculated the times of the phase maxima which are relatively sharp features. In the case of the amplitude variations, we calculated both the amplitude maxima and the times when the $A(t)$ curves crossed the 0.1-magnitude level (the approximate mean light level) upwards. The latter, arbitrary point on the rising branch can be measured more accurately than the maxima.

All three measures of the cycle length of the primary modulation in Fig. 11 indicate that the modulation period is indeed changing. Although the $O-C$ variation of the phase and amplitude maxima is marginal due to the large uncertainties, the phase and period agrees with the secondary modulation we detected in the phase variations of the pulsation (Fig. 9). The mean brightness levels on the rising branch on the other hand can be determined more accurately and fit to the variations as well. The amplitudes are somewhat different: the times of the amplitude maxima vary by 115 ± 12 days (about 9.5%) whereas the times of the phase maxima vary by 172 ± 51 days or about 14%. The average period of the primary modulation was found to be $P_{m1}(A(t)) = 1209.7 \pm 8.2$ d and $P_{m1}(\phi(t)) = 1188 \pm 35$ d, in agreement with the results of the Fourier analysis. If we allow the secondary modulation period to be fitted, the amplitude data results in a period of $P_{m2} = 5330 \pm 137$ days. The phase data provide only a very uncertain period.

The variations of the primary modulation period indicate that the modulations may possibly interact with each other. Benkő et al. (2011) argue that two parallel, independent modulating waves are unlikely to occur in real stars without interaction. According to their mathematical formulation, in the case of an amplitude and/or frequency modulation cascade, linear combinations of the two modulation frequencies should be present at the low-frequency end of the Fourier spectrum. However, the data is insufficient to detect f_{m2} itself or its combinations with f_{m1}. Unfortunately, the combination peaks between the side-peaks can arise simply from the presence of the two frequency modulations and their presence cannot distinguish between independent and interacting modulations. The current time span of the data covers only two and a half secondary modulation cycles, therefore further long-term monitoring will be necessary to detect the signs of any interaction.

The periodic variations in the length of the primary modulation cycle may explain the different values found in the literature: e.g., Cabanela (1991) determined P_{m1} to be 1258 days but his data covered mostly the time interval of significantly longer modulation period around JD 2445000.

6.3 Comparison with the radial velocity

We collected a limited amount of RV measurements from the literature as well (Fig. 1). We calculated the amplitude and phase variations of the data in the same manner as we did for the photometry. The results revealed that the RV exhibits the same amplitude modulation. We calculated the $q = A_{v_{\rm rad}}/A_B$ parameter to confirm that the star pulsates in the second overtone (Fig. 3). We also scaled the amplitude variations to the V-band photometric amplitude values in Fig. 12 with a scaling factor of $A_{v_{\rm rad}}/A_V = 83$. The lower panel of Fig. 12 shows that the phase follows the same overall slopes as the photometric data but very little data are available at the maximum phase peaks.

In lack of Burki's much more extended RV data, we were

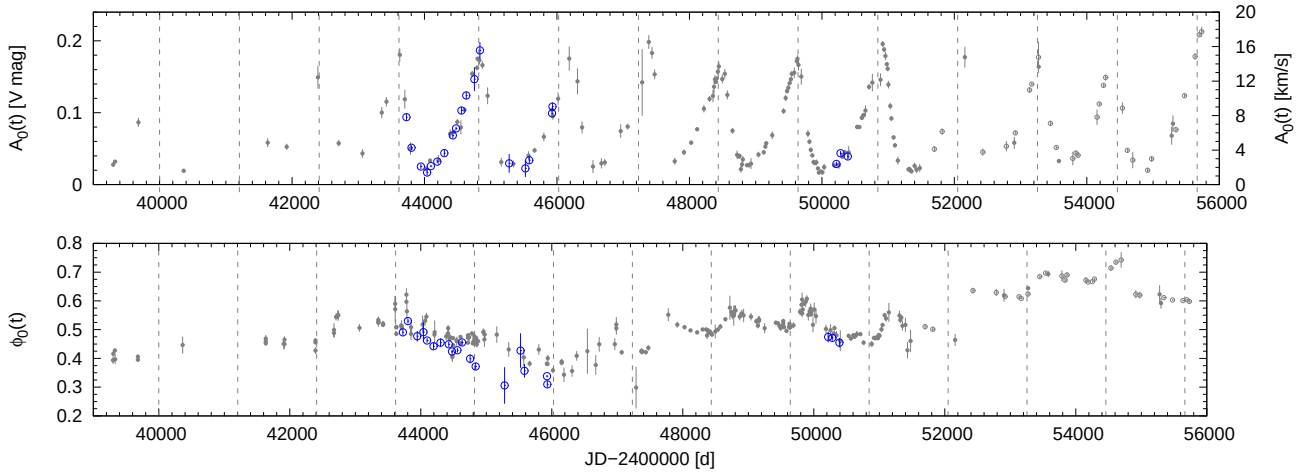

Figure 12. Top panel: blue circles represent the amplitude variations of the radial velocities, scaled as indicated in Sect. 6.3, grey points are the amplitude variations of the photometric data (same as the blue points in Fig. 8). Bottom panel: the same for the phase variations. Grey vertical lines mark the modulation cycles with a spacing of 1205 days.

not able to investigate whether the secondary modulation is present in the amplitudes and phases of the RV measurements. A visual inspection of Figure 5 in Burki (2006) hints at a slight decrease in the maximum amplitudes from about JD 2446500 until JD 2449000, in accordance with our findings. However, we cannot exclude that the data set simply misses the largest-amplitude pulsation cycles.

However, we can compare his phase variation results with our calculations. The values were extracted from the original figure with the DEXTER online tool[2] so the timings are not accurate enough to analyse the data but they make a visual comparison possible. Burki (2006) noted that the phase seems to experience sudden jumps. If we transform our data to the pulsation frequency used in that paper ($f = 0.6707073\,\mathrm{d}^{-1}$), the similarities become evident. As Fig. 13 shows, the apparently flat sections of the phase variations are the combined result of the selected pulsation period, the shape of the phase modulation curve with the sharp peaks at maximum values and the fact that some of these peaks are not sampled by Burki (2006). This figure provides further hints that the secondary modulation is present in the RV variations: the change of slope at JD 2446200 coincides with one of the minima in the phase variation in Fig. 9.

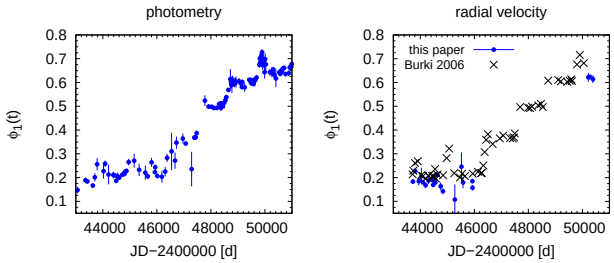

Figure 13. Comparison of our phase variation results and the RV phase variations obtained by Burki (2006). Here the basic pulsation frequency is $f = 0.670703$ instead of the $f = 0.670775$ value we used in the rest of the figures. Blue points: data used in this paper, grey crosses: data points extracted from Burki (2006).

6.4 Comparison with RR Lyrae stars

An important issue is to determine the level of similarity or difference to the Blazhko effect observed in RR Lyrae stars. Multiple modulation cycles were identified in several Blazhko stars, both from ground- and space-based measurements (Sódor et al. 2011; Guggenberger et al. 2012), although the occurrence rate was found to be widely different. The *Kepler* sample used by Benkő et al. (2014) is relatively small with only 15 stars, but the ultra-precise photometry revealed multiple modulation in 80% of the sample. Ground-based survey data yielded 12%, based on a larger sample (12/100 stars) but with much less precision and temporal coverage, therefore this result should be considered as a lower limit (Skarka 2014). In any case, multiple modulation is not unexpected for RR Lyrae stars.

The primary modulation is relatively slow compared to the pulsation period ($P_{m1}/P_{\mathrm{puls}} \approx 808$). However, slow modulation is not uncommon among RR Lyrae stars either: the largest period ratio in the *Kepler* sample is $P_m/P_{\mathrm{puls}} = 723/0.5617 = 1287$ for V454 Lyr (KIC 6183128). Stars with modulation periods up to about 3000 days were identified in the OGLE-III data (Soszyński et al. 2011).

As Fig. 6 shows, the shape of the primary amplitude modulation is highly asymmetric. Such modulation envelopes are uncommon but not unprecedented among RR Lyrae stars: *e.g.* the stars RX Col and FS Vel display a slowly increasing pulsation amplitude, followed by a fast decrease towards the minimum amplitude (Skarka 2014).

Another possibility for comparison is the phase relation between the pulsation amplitude and phase variations. Blazhko RR Lyrae stars show a wide variety of modulation relations. If plotted as a loop diagram (e.g. $\phi_1(t)$ plotted against $A_1(t)$), the shape of the loops and the direction of progression indicate the relation of the two measurements. We presented a loop diagram for V473 Lyrae in our pre-

[2] http://dc.zah.uni-heidelberg.de/sdexter

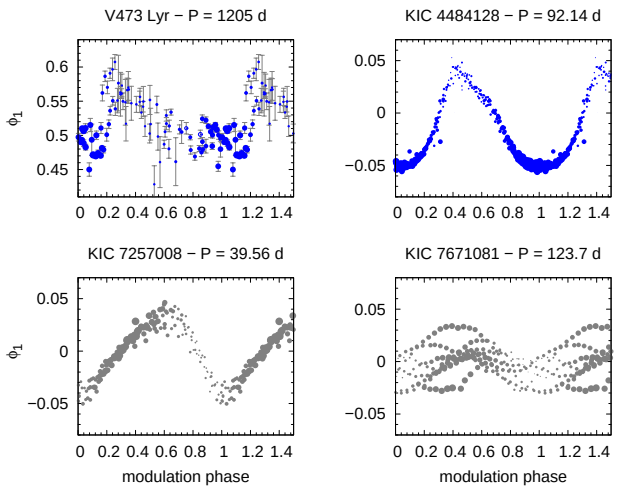

Figure 14. Comparison of the amplitude and phase modulations between V473 Lyrae and three RR Lyrae stars. Positions of the points indicate the $\phi_1(t)$ value, point sizes the corresponding $A_1(t)$ value. All three RR Lyrae stars are from the *Kepler* sample (Benkő et al. 2014). KIC 4484128 (V808 Cyg) shows similar variations while KIC 7257008 and KIC 7671081 (V450 Lyr) display very different curves. Modulation periods are indicated.

vious paper (Molnár et al. 2013). The visualization of the loops of the star, however, required additional smoothing. Here we follow a different method and plot the phase variations instead, folded by the (primary) modulation period. The corresponding pulsation amplitude values are then indicated with the sizes of the points (Fig. 14).

We selected three RR Lyrae stars from the *Kepler* sample for comparison (Benkő et al. 2014). Two stars (KIC 7257008 and KIC 7671081, bottom row) display very different modulations. In the case of the former star, a roughly quarter-period shift is evident between the amplitude and phase, *i.e.* maximum and minimum amplitudes occur around the middle of the rising and descending branches of the phase variations. In the latter case, the relation between the amplitude and phase modulations themselves varies over time. The third star (KIC 4484128, V808 Cyg), however, shows variations similar to V473 Lyr (top row) with antiparallel phase and amplitude variations (which translates to parallel amplitude and $O-C$ variations). These examples, together with the asymmetry and length of the primary modulation and the presence of the secondary modulation indicate that analogues to V473 Lyrae can be found among the RR Lyrae stars. We must point out, however, that they also indicate that the variations collectively referred to as the Blazkho effect itself is a very diverse phenomenon.

7 HYDRODYNAMIC MODELS

Currently the most plausible model of the Blazhko effect is the mode resonance hypothesis (Buchler & Kolláth 2011). Given that the pulsation of RR Lyrae stars and Cepheids share many similarities, one can expect that mode resonances occur in Cepheids too. To find out, we calculated a large set of linear hydrodynamic models with the Florida-Budapest code (Kolláth & Buchler 2001; Kolláth et al. 2002). Initial fundamental parameters (effective temperature, mass, luminosity) were based on earlier results from the literature.

Fabregat et al. (1990) derived these parameters from *uvbyβ* photometric observations and found that $T_{\rm eff} = 5860\pm100\,K$, $L = 960\pm390\,L_\odot$ and $M = 4.1\pm2.5\,M_\odot$. Based on spectroscopic observations and comparison with previous studies, Andrievsky et al. (1998) determined the parameters to be $T_{\rm eff} = 6100\,K$, $L = 740\,L_\odot$ with pulsational and evolutionary masses of $M_{\rm puls} = 3.0\,M_\odot$ and $M_{\rm evol} = 4.6\,M_\odot$. Therefore our model grid was set up with the following limits and steps: $M = 4-5\,M_\odot$, $0.1\,M_\odot$; $T_{\rm eff} = 5800-6400\,K$, $25\,K$; $L = 720-950\,L_\odot$, $5\,L_\odot$ and a chemical composition of $X = 0.70$; and $Z = 0.016$.

We searched the model grid for resonances between the linear periods of the second overtone and other radial modes. The results are summarized in Fig. 15. The plots are similar diagnostic diagrams that were created for RR Lyrae models by Kolláth, Molnár & Szabó (2011). The resonant solutions spread out to a relatively flat surface in the three-dimensional $T_{\rm eff} - M - L$ parameter space. A well-chosen 2D projection of this space reduces the subspace of resonant models into a relatively thin strip thus making the visualization much easier. For RR Lyrae stars, the projection was $T_{\rm eff}$ *vs.* $150\,M - L$ where M and L are in solar units. For the much more luminous Cepheids, the projection was found to be $500\,M - L$, in solar units (Fig. 15).

7.1 Linear resonances

A main difference from the RR Lyrae study of Kolláth et al. (2011) is that V473 Lyr is pulsating in the second overtone instead of the fundamental mode. Therefore period ratios with the higher modes are very different. Antonello & Kanbur (1997) noted that the $P_2/P_6 = 2$ resonance can occur with the sixth overtone in their radiative nonlinear second-overtone models. However, Moskalik & Buchler (1990) showed that in W Vir models, only the half-integer resonances destabilize the pulsation mode, and the same was observed in RR Lyrae models Kolláth et al. (2011). For the RR Lyrae models several half-integer ($(2n+1)/2$) resonances that occur with a whole spectrum of overtones were identified. In contrast, we could find only two cases for the second-overtone Cepheid models, as seen in panel A of Fig. 15: a 3:2 resonance with the 4th overtone and a 5:2 resonance with the 8th overtone. In the plot we selected models with period ratios that are within ±0.1% from the exact resonance value.

From the two cases, the 8th overtone is more interesting: it may be a strange mode, *i.e.* it can be trapped in the uppermost layers of the star and alter the pulsation significantly. Such interaction was recently observed in RR Lyrae stars where a resonance between a strange mode and the fundamental mode causes a period doubling bifurcation in the pulsation (Szabó et al. 2010; Kolláth et al. 2011).

Although the 8th overtone is a good candidate for the mode-resonance induced instability of the pulsation, we looked for other resonances too. Panel C in Fig. 15 shows the locations of the quarter-integer ($(2n+1)/4$) resonances. In this case, we identified five possibilities: resonances with 1st, 3rd, 5th, 7th and 9th overtones.

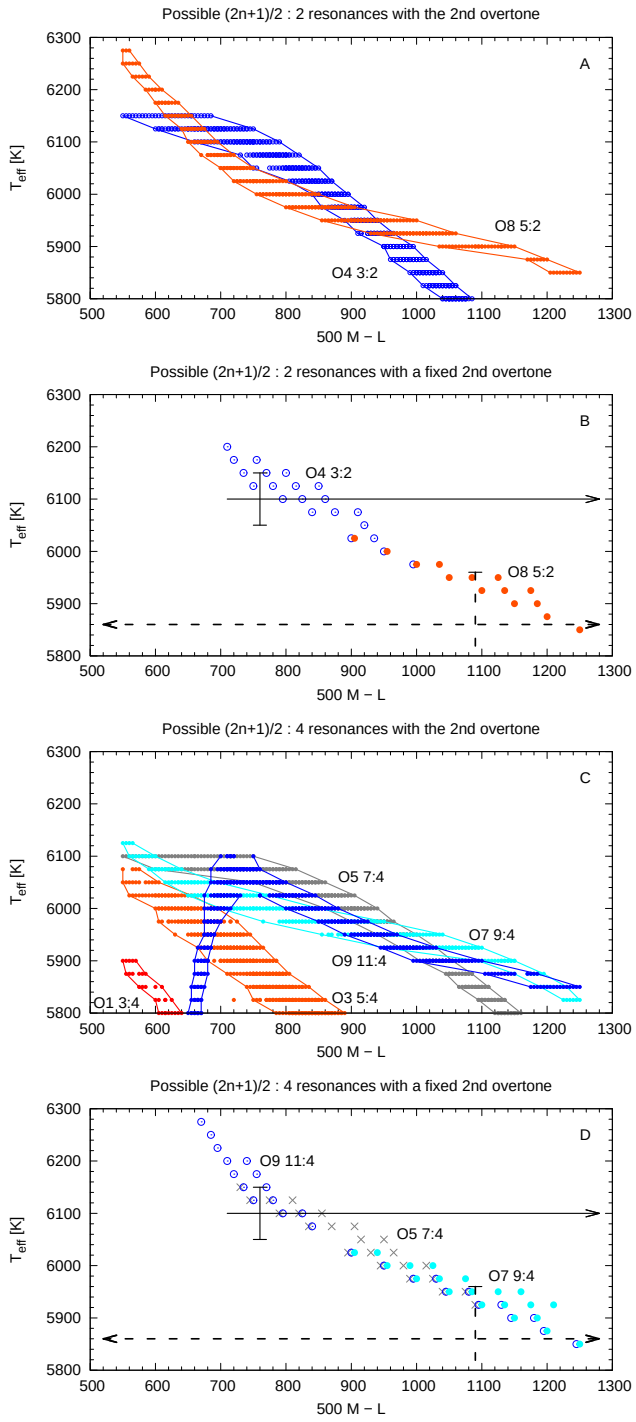

Figure 15. The diagnostic diagram of the linear hydrodynamic Cepheid models. Resonance regions are plotted in a 2D projections of the original $T_{\rm eff} - M - L$ space. Mass and luminosity values are in solar units. The black crosses and arrows indicate the possible positions of V473 Lyrae. A: half-integer resonances with the second overtone. B: solutions close to half-integer resonances with the second overtone fixed at $P = 1.4909$ d. C: quarter-integer resonances. D: solutions close to quarter-integer resonances with a fixed overtone period.

Focusing now on V473 Lyrae, there is an additional constraint to the models: the pulsation period. In panels B and D we only plotted the solutions that are both close to the resonances and close to the period of the second overtone ($P_2 = 1.485 - 1.492$ d). Since nonlinear models can lock into resonances even if the period ratios of the linear models are slighly off, we extended the allowed period ratio range to $\pm 0.5\%$. The fundamental parameters of Fabregat et al. (1990) and Andrievsky et al. (1998) are also indicated with dashed and continuous lines, respectively. In the former case for the mass we used the $M_{\rm puls} = 3.0\,M_{\odot}$ value. The two positions of the star align well with the selected models but select different resonances.

However, there are complications to these results. Large uncertainties in the luminosity and especially in the mass of the star make the $500M - L$ parameter very vague. The experiences with RR Lyrae models also tell us that metallicity can shift the position of the resonant solutions in the diagram considerably (Kolláth et al. 2011). The difference between the linear and nonlinear mode frequencies also shifts the region of nonlinear resonant models compared to the linear ones. Therefore the linear models only tell us that there indeed are plausible resonances to drive the modulation but only further research will be able to reveal which, if any, may be operating in V473 Lyrae. The effects of different metallicities and the analysis of the nonlinear models will be detailed in a separate paper.

8 CONCLUSIONS AND FUTURE WORK

We examined the photometric data of the Cepheid V473 Lyrae collected by various observers and covering about 44 years in several photometric bands. The star shows strong amplitude and phase modulations with an average period of $P_{m1} = 1205 \pm 3$ days. With the help of the limited amount of RV measurements at hand, we also confirmed that the star is pulsating in the second overtone. We identified modulation side-lobes up to the third order (septuplets).

It turned out, however, that the light variations of the star are even more complex. After a careful analysis we identified a secondary modulation both in the Fourier spectra and the amplitude and phase variations of the star. This tertiary period of the star is in the range of $P_{m2} = 5300 \pm 150$ days, or 14.5 years and detectable in both the amplitude and phase variations. Recent results revealed that multiple modulations not only occur (Skarka 2014) but they may prevail in Blazhko stars (Benkő et al. 2014). We also detected that the length of the primary modulation cycle changes in parallel with the secondary cycle. We expect that the two cycles interact with each other but the current amount of data is insufficient to decide this question.

Phenomenologically, we consider the light curve variations of V473 Lyrae equivalent with the Blazhko effect. Although some details, such as the asymmetry of the primary modulation or the relation of the amplitude and phase variations seem to differ from the general picture, we can find an RR Lyrae counterpart for each particular aspect. This fact underlines that the Blazhko effect is a very diverse phenomenon and without physical models, the similarities remain convincing but not conclusive.

There are several open questions that deserve further

attention. These ground-based data lack the precision to identify low-amplitude additional modes that may drive mode interactions in the star. In RR Lyrae stars, space-based photometry revealed that almost all modulated stars show additional frequency components in the Fourier spectra at the millimag level (Benkő et al. 2010). Continuous coverage was crucial to the discovery of period doubling (Szabó et al. 2010). Currently the only space-based photometer that can observe V473 Lyr is the Canadian MOST satellite (Walker et al. 2003). We successfully applied for telescope time and MOST will observe the star for one month in July 2014. Although one month is a very short time compared to the modulation cycles, the continuous and precise monitoring of the star will be essential to identify additional modes and cycle-to-cycle variations (assuming that they will be present during those $\sim$ 20 pulsation cycles). The TESS space telescope[3], to be launched in 2017, will also observe the star for one month.

Continued follow-up of the modulation cycles is also important. On the one hand, our analysis was limited by the strongly varying temporal coverage and photometric precision, the use of different filters and the systematic differences that are inherent to the data combined from several sources. On the other hand, the star is too bright for most automated survey telescopes. A new initiative, however, may provide extended, homogeneous measurements of the star. The Fly's Eye[4] project will use 19 small, wide-field cameras to provide a high-cadence, multicolour time-domain survey of the entire visible sky down to 30 degrees altitude (Pál et al. 2013). The prototype of the system may start observing the star from this year on. We also encourage amateur astronomers to follow the star's light variations with digital photometry.

Finally, non-linear hydrodynamic modelling of second-overtone Cepheids will be vitally important to determine whether mode resonances occur in these stars. Recent advancements in 1D pulsation codes revealed that both RR Lyrae and BL Herculis (short period Type II Cepheid) models may exhibit multimode pulsation, mode resonances, chaos, and small-amplitude modulation (Kolláth et al. 2011; Molnár et al. 2012; Plachy, Kolláth & Molnár 2013; Smolec & Moskalik 2012, 2014). If mode interactions can be identified in second-overtone Cepheid models, they will undoubtedly support the case of the mode resonance model, and will point towards a unified model for the Blazhko effect in Cepheid and RR Lyrae stars.

ACKNOWLEDGEMENTS

We thank the referee, Shashi Kanbur, for his comments that helped to improve the paper. Fruitful discussions with József Benkő are gratefully acknowledged. The work of L. Molnár leading to this research was supported by the European Union and the State of Hungary, co-financed by the European Social Fund in the framework of TÁMOP 4.2.4. A/2-11-1-2012-0001 'National Excellence Program'. This work has been supported by the Hungarian OTKA grant K83790, the ESTEC Contract No. 4000106398/12/NL/KML, and the 'Lendület-2009' Young Researchers' Programme of the Hungarian Academy of Sciences. We acknowledge the AAVSO International Database contributed by observers worldwide.

[3] http://space.mit.edu/TESS
[4] http://www.flyseye.net

REFERENCES

Andrievsky S. M., Kovtyukh, V. V., Bersier D., Luck, R. E., Gopka, V. P., Yushchenko A. V., Usenko, I. A. 1998, A&A, 329, 599
Antonello E., Kanbur, S. M. 1997, MNRAS, 286, L33
Arellano Ferro A. 1984, MNRAS, 209, 481
Arellano Ferro A., Parrao L., Schuster W., González Bedolla S., Peniche R., Pena J. H. 1990, A&AS, 83, 225
Auvergne M. 1986, A&A, 159, 197
Balona L. A., Stobie R. S. 1979, MNRAS, 189, 649
Benkő J. M., Szabó R., Paparó M. 2011, MNRAS, 417, 947
Benkő J. M. et al. 2010, MNRAS, 409, 1585
Benkő J. M. et al. 2014, ApJS, submitted
Berdnikov L. N. 2008, VizieR On-line Data Catalog, 2285, 0
Berdnikov L. N., Pastukhova, E. N. 1994, AstL, 20, 720
Berdnikov L. N., Ignatova V. V., Pastukhova E. N., Turner D. G. 1997, AstL, 23, 177
Breger M. 1969, ApJS, 19, 79
Breger M. 1981, ApJ, 249, 666
Breger M. 2006, CoAst, 148, 52
Buchler J. R., Kolláth Z. 2011, ApJ, 731, 24
Buchler, J. R., Yecko P., Kolláth Z. 1997, A&A, 326, 669
Burki, G. 1984, IAUS, 105, 45
Burki G. 2006, JAAVSO, 35, 19
Burki G., Mayor M. 1980a, IBVS, 1728, 1
Burki G., Mayor M. 1980b, A&A, 91, 115
Burki G., Mayor M., Benz W. 1982, A&A, 109, 258
Burki G., Schmidt E. G., Arellano Ferro A., Fernie J. D., Sasselov D., Simon N. R., Percy J. R., Szabados L. 1986, A&A, 168, 139
Cabanela J. E. 1991, JAAVSO, 10, 54
Cousins A. W J., Caldwell J. A. R. 1985, Obs., 15, 134
Csubry Z., Kolláth Z. 2004, in Danesy D., ed., Proc. SOHO 14/GONG 2004 Workshop, Helio- and Asteroseismology: Towards a Golden Future, ESA SP-559, ESA, Noordwijk, p. 396
Detre L., Szeidl B. 1973, IBVS, 764, 1
Eggen O. J. 1985, AJ, 90, 1297
Engle S. G., Guinan E. F. 2013, AAS Meeting 221, 354.18
ESA 1997, The Hipparcos and Tycho Catalogues, ESA SP-1200, Noordwijk
Fabregat J., Suso J., Reglero V. 1990, MNRAS, 245, 542
Fernie J. D. 1982, PASP, 94, 537
Guggenberger E. et al. 2012, MNRAS, 424, 649
Henriksson G. 1983, Uppsala Obs. Rep., No. 26
Ignatova, V. V., Vozyakova, O. V. 2000, A&AT, 19, 133
Klagyivik P., Szabados L. 2009, A&A, 504, 959
Kiss, L. L. 1998, MNRAS, 297, 825
Koen C. 2001, MNRAS, 322, 97
Kolláth Z., Buchler J. R. 2001, in *Stellar Pulsation – Nonlinear Studies*, ASSL, vol. 257, pp. 29-60, Kluwer, Dordrecht
Kolláth Z., Buchler J. R., Szabó R., Csubry Z. 2002, A&A, 385, 932

Kolláth Z., Molnár L., Szabó R. 2011, MNRAS, 414, 1111
Lenz P., Breger M. 2005, CoAst, 146, 53
Molnár L., Kolláth Z., Szabó R., Plachy E. 2012, AN, 333, 950
Molnár L., Szabados L., Dukes R. J. Jr., Győrffy Á., Szabó R. 2013, AN, 333, 980
Moskalik P., Buchler J. R. 1990, ApJ, 355, 590
Moskalik P., Kołaczkowski Z. 2009, MNRAS, 394, 1649
Ogłoza W., Moskalik P., Kanbur S. 2000, in ASPC 203, The Impact of Large-Scale Surveys on Pulsating Star Research, eds. L. Szabados, D. W. Kurtz (San Francisco: ASP), p. 235
Oja T. 2011, JAD, 17, 1
Pál A. et al. 2013, AN, 334, 932
Percy J. R., Evans N. R. 1980, AJ, 85, 1509
Percy J. R., Baskerville I., Trevorrow D. W. 1979, PASP, 91, 368
Plachy E., Kolláth Z., Molnár L. 2013, MNRAS, 433, 3950
Pojmanski G. 2002, AcA, 52, 397
Simon N. R., Lee A. S. 1981, ApJ, 248, 291
Skarka M. 2014, A&A, 562, 90
Smolec R., Moskalik P. 2012, MNRAS, 426, 108
Smolec R., Moskalik P. 2014, MNRAS, 441, 101
Smolec R. et al. 2012, MNRAS, 419, 2407
Sódor Á. et al. 2011, MNRAS, 411, 1585
Soszyński I. et al. 2010, AcA, 60, 17
Soszyński I., Dziembowski W. A., Udalski A. et al. 2011, AcA, 61, 1
Stothers R. B. 2009, ApJ, 696, L37
Szabó R. 2014, IAUS, 301, 241
Szabó R. et al. 2010, MNRAS, 409, 1244
Szeidl B., Jurcsik J. 2009, CoAst, 160, 17
Van Hoolst T., Waelkens C. 1995, A&A, 295, 361
Walker G. et al. 2003, PASP, 115, 1023
Williams J. A. 1966, AJ, 71, 615
Wozniak P. R., Williams S. J., Vestrand W. T., Gupta V. 2004, AJ, 128, 2965